Journal of Engineering Science and Technology
Vol. 18, No. 6 (2023) 3077 - 3096
© School of Engineering, Taylor's University

PREDICTIVE ANALYTICS OF JUNCTIONLESS DOUBLE GATE STRAINED MOSFET USING GENETIC ALGORITHM WITH DOE-BASED GREY RELATIONAL ANALYSIS

K. E. KAHARUDIN[1,2], F. SALEHUDDIN[1,*], N. A. JALALUDIN[1], F. ARITH[1], A. S. M. ZAIN[1], I. AHMAD[3], S. A. M. JUNOS[1]

[1]Micro & Nano Electronics (MiNE), CeTRI, Faculty of Electronics and Computer Technology and Engineering, Universiti Teknikal Malaysia Melaka, Hang Tuah Jaya, Durian Tunggal, 76100 Melaka, Malaysia
[2]Faculty of Engineering, Lincoln University College (Main Campus), Wisma Lincoln, 47301 Petaling Jaya, Selangor, Malaysia
[3]College of Engineering (CoE), Universiti Tenaga Nasional (UNITEN), 43009 Kajang, Selangor, Malaysia
*Corresponding Author: fauziyah@utem.edu.my

Abstract

This paper explores the application of Genetic Algorithm (GA) incorporated with design of experiment (DoE) based on Grey Relational Analysis (GRA) in predicting the optimal design parameters of n-type Junctionless Double Gate Strained MOSFET (JLDGSM). The GRA is applied to predict the optimum level of multiple design parameters in attaining the best multiple device characteristics. The GA approach is applied to further optimize the design parameters for much improved device characteristics. The initial step is to select the best possible level of four design parameters (Ge mole fraction, high-k material thickness, source/drain doping concentration and metal work-function) within specific upper and lower boundary limits. The predictive analytics are initiated with the employment of GRA in finding the grey relational grade (GRG) which represents the multiple electrical characteristics (I_{ON}, I_{OFF}, *on-off ratio*, g_m, f_T *and* f_{max}) for 18 sets of experiment. The computed GRGs are then processed using multiple regression analysis to derive the objective function that summarizes the relationship between the design parameters and the GRG. Finally, the genetic algorithm is utilized to predict the optimum level of design parameters based on the derived objective function. The final result reveals that the proposed predictive analytics have successfully optimized I_{ON}, I_{OFF}, *on-off ratio*, g_m, f_T and f_{max} of the device by ~34%, ~40%, ~50%, ~18%, ~10% and ~4% respectively. The best combinational magnitudes of Ge mole fraction, $T_{high\text{-}k}$, N_{sd} and WF for the most optimum device characteristics are predicted to be 0.1 (10%), 3 nm, 3×10^{13} cm^{-3} and 4.6 eV respectively. The results exhibits significant potential for junctionless transistor revealing the alternative way and configuration in developing future highly efficient nano-scaled devices and ion-sensitive sensors.

Keywords: Maximum oscillation frequency, Off-current, On-current, On-off ratio transconductance, Unity-gain frequency.

1. Introduction

For recent generations, the size of transistors have been rapidly scaled down in accordance with the Moore’s law forecast in which the number of transistors on a microprocessor doubles every two years, yet the cost of computers is half. Moore's law also implies that the speed and capabilities of computers to rise every couple of years, resulting in them becoming cheaper. The scaling of the transistor brings substantial benefits to the microprocessor industry, such as reduced production costs, faster data transmission speeds, and high frequency applications. Variations in parameters pose the greatest challenge to shrinking the transistor's size. During the manufacturing process, alterations in parameters like as size, oxide thickness, doping concentrations, strained-silicon effects, diffusion depth, and channel length may affect the electrical and physical characteristics of devices and circuits. Quasi transistor characteristics result in timing fluctuations in circuit critical routes, narrower read/write noise margins for memory cells, and larger off-state leakage currents, which ultimately lead to performance degradation. To accommodate for performance losses generated by parameter fluctuations, circuits must often be built conservatively, demanding devices with a greater area and higher power consumption. To prevent excessively gloomy designs, it is crucial to comprehend and measure process-induced unpredictability. Designers may maximize performance, power, area, and yield by improving the analysis and modelling of variability.

Swami and Rai [1] examined the impact of physical parameter variations on DG-MOSFET performance characteristics. Quantum confinement of charge carriers dramatically affects the performance characteristics (mostly the subthreshold features) of the device, and hence cannot be neglected in the design of subthreshold region-based circuits. Bala et al. and Kumar [2] showed that dopingless nanotube MOSFET has low on-current and less sensitivity towards multiple design parameter fluctuations than extensively-doped junctionless nanotube MOSFET. It was noticed that the subthreshold slope (SS), DIBL, I_{ON} and I_{OFF} current of the junctionless device showed greater sensitivity to gate length variations as compared to dopingless device. Hence, it is extremely vital having a specific method to lessen sensitivity on design parameter of junctionless transistors. Batakala and Dhar [3] explored the effect of channel material on the performance characteristics of GAA MOSFET which revealed that the channel length is a crucial controllable parameter for minimizing the output fluctuations of transistors.

A new n-MOS Graded Channel Double Gate layout proposed by Wagaj and Patil [4] indicated that when the side gate voltage is increased, the surface potential likewise rises, resulting in an increase in current driving capacity. Additionally, junctionless structure boosts the transconductance by a factor of three. This is mostly because the channel region of junctionless transistors is strongly and consistently doped from source to drain region, causing a high scattering mechanism that results in nearly negligible electric fields at the channel's core, which is advantageous for charge carrier mobility. Sinha [5] presents a simulation-based analysis of a double gate graded channel junctionless MOSFET with channel engineering approach. The finding indicates that the change in potential to one side and deeper diminished off-state current without impacting the on-state current. In a junctionless structure, the threshold voltage decreases with temperature more gradually than in a typical device. This implies that doping concentration and workfunction are considered key design factors that must be statistically optimized to reduce output fluctuations.

Universities, research institutes and semiconductor manufacturers have conducted a significant number of studies dealing with random parameter distributions. Historically, the effect of random dopant distributions on fluctuations in threshold voltage was analysed using a simple mathematical model [6]. Asenov et al. [7-9] thoroughly investigated the influence of random dopant distributions on threshold voltage using a 3D atomistic modelling technique. It is well established that random dopant distributions resulting from the doping engineering process are the primary source of statistical variation in nanoscale transistor devices [10-12]. The application of Design of Experiment (DoE) approach is one of the methodological approaches for addressing this issue. For example, response surface methodology (RSM) was utilized to investigate the effect of design parameter variations on threshold voltage for multiple technology node ranges [13-15]. It has been demonstrated that the RSM approach consumes less time with device simulations than the Monte Carlo method when evaluating the variability of design parameters in relation to threshold voltage variations [16].

Taguchi design, in addition to RSM, is a well-known approach that leverages DoE to investigate and optimize many design parameters of different transistor configurations [17-20]. Taguchi design utilizes an orthogonal array (OA) that simplifies and shortens experiment runs. In dealing with multi-objective issues, Taguchi design and Grey relational analysis (GRA) are frequently integrated. GRA is an analytical method that combines and transforms various output qualities into a single representative grade. Numerous studies shown that hybrid Taguchi-GRA design may address multi-objective optimization issues in a variety of engineering disciplines [21-23]. Although the hybrid Taguchi-GRA design may simultaneously optimize many design parameters for multi-objective optimization problems, it is restricted to finding optimal solutions within the level of design parameters specified. In order to compensate for this deficiency, metaheuristic approaches such as the Genetic algorithm have been utilized [24-26]. This work describes the predictive analytics of Junctionless Double Gate Strained MOSFET (JLDGSM) using Genetic Algorithm with DoE-based Grey Relational Analysis.

Inspired by the aforementioned research on MOSFET's performance, this articles aims to use Genetic Algorithm with Design of Experiments-based Grey Relational Analysis to forecast the behaviour of JLDGSM device. Listed below are the most important contributions to this work:

- We design, simulate and analyse the n-type JLDGSM with 6nm of physical gate length (L_g). The device demonstrates high source-drain current (I_{ds}), acceptable off-state current (I_{OFF}) and good on-off ratio.
- We propose a hybrid predictive analytics consisting of Genetic Algorithm with DoE-based Grey Relational Analysis as a method to find the optimum input parameters of n-type JLDGSM in attaining better output characteristics. The optimized JLDGSM demonstrates better on/off-state current, on-off ratio, maximum oscillation frequency, transconductance and unity-gain frequency.

This articles is structured as follows: Section 2 describes the simulation of the JLDGSM's process and devices. In Section 3, the predictive analytics of the device utilizing Genetic Algorithm with DoE-based Grey Relational Analysis is described. This study's results and discussion are presented in Section 4. Section 5 concludes with a brief summary of this study's results.

2. Process and Device Simulation

The n-type JLDGSM transistor was designed and modelled using industrial-based simulation software, Silvaco TCAD tools in which the process and device simulations were carried out using Athena and Atlas module respectively. The process simulation utilized silicon germanium (SiGe) material with <100> orientation as the main substrate with Germanium (Ge) mole fraction was set at 0.3 (30%). Previous publications [27] on the subject of process simulation might be consulted for insight about its detailed procedures. The full structure of the n-type JLDGSM transistor was completed by reflecting the left-hand side and upper side structure as depicted in Fig. 1. Table 1 summarizes the initial magnitude of the investigated design parameters that will be manipulated for the predictive analytics of the n-type JLDGSM performance.

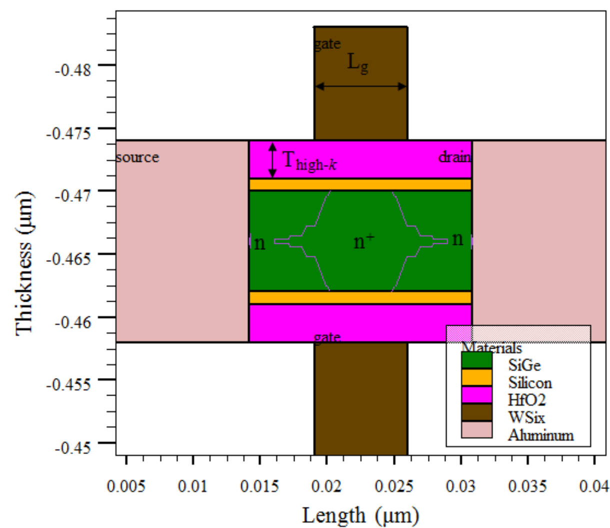

Fig. 1. Cross-sectional structure of n-type JLDGSM device.

Table 1. Initial magnitude of design parameters for n-type JLDGSM.

Design Parameters	Units	Magnitude
Ge mole fraction in SiGe layer	-	0.3 (30%)
High-k material Thickness, $T_{high\text{-}k}$	nm	2
S/D Doping, N_{sd}	cm^{-3}	1.0E13
Metal Workfunction (*WF*)	eV	4.7

The I_{ds}-V_{gs} curve will be generated at a constant drain-to-source voltage (V_{ds}) = 0.5 V as the gate-to-source voltage (V_{gs}) is shifted from 0 V to 1 V. The initial on-current (I_{ON}) and the off-current (I_{OFF}) of the n-type JLDGSM transistor can be extracted from the transfer curve. Besides that, the *on-off ratio* is also an important characteristic used to indicate the power consumption of the device. Larger *on-off ratio* indicates the transistor has better power consumption. The initial *on-off ratio* of the n-type JLDGSM transistor can be calculated as:

$$On - Off\ ratio = \frac{I_{ON}(I_{ds}\ when\ V_{gs}=1V)}{I_{OFF}(I_{ds}\ when\ V_{gs}=0V)} \tag{1}$$

Furthermore, the transconductance (g_m) of the transistor can be calculated based on the data extracted from I_{ds}-V_{gs} transfer characteristics. The g_m magnitude is very important characteristic in amplifier's designs, and it can be measured as:

$$g_m = \frac{\partial I_{ds}}{\partial V_{gs}} \quad (2)$$

In term high frequency performance, unity-gain frequency (f_T) and maximum oscillation frequency (f_{max}) are the main characteristics that have to be taken into account for design consideration. Higher magnitude in f_T and f_{max} implies the better suitability of the device to operate in high frequency RF application. The extraction of intrinsic capacitances (C_{gs} and C_{gd}) are very crucial to calculate the magnitude of f_T and f_{max}. Thus, AC small signal analysis was performed after post-processing DC analysis. By extracting the magnitude of C_{gs} and C_{gd} from the curve, the f_T and f_{max} of the n-type JLDGSM transistor can be calculated as follows:

$$f_T = \frac{g_m}{2\pi(C_{gs} + C_{gd})} \quad (3)$$

$$f_{max} = \sqrt{\frac{f_T}{8\pi R_g C_{gd}}} \quad (4)$$

where,

$$R_g = \frac{1}{2\pi f_T(C_{gs} + C_{gd})} \quad (5)$$

3. Predictive Analytics

The optimum level of the four design parameters (Ge mole fraction, $T_{high\text{-}k}$, N_{sd} and *WF*) for equitable transistor characteristics (I_{ON}, I_{OFF}, *on-off ratio*, g_m, f_T and f_{max}) were predicted using the proposed predictive analytics. The predictive analytics involved three main stages which were; 1) Grey Relational Analysis; 2) Multiple Regression Analysis; 3) Genetic Algorithm. Figure 2 shows the general flowchart of the steps involved in the proposed predictive analytics.

3.1. Grey relational analysis

Grey relational analysis (GRA) was originally introduced by Ju Long in 1982 [28]. The application of GRA relies on a specific concept of information that aid to analyse the incomplete or uncertain data [29]. The GRA is often regarded as a method to search the balanced solution for a certain system. It does not offer the best solution but does provide a tolerable solution for multi-objective problems. In this study, the GRA was carried out by analytically evaluating the relation between the investigated electrical characteristics and their corresponding problems.

The GRA was utilized to compute the Grey relational grade (GRG) for 18 sets of DoE in which all the parameter levels were evenly distributed in each column. The investigated design parameters (represented by x_1, x_2, x_3 and x_4) were varied into three multiple magnitudes as shown in Table 2. The main objective of GRA was to compute the GRG for each experiment rows in regard with the corresponding electrical characteristics and the types of problem. In other words, the function of GRA was to convert the multiple transistor characteristics (I_{ON}, I_{OFF}, *on-off ratio*, g_m, f_T and f_{max}) with different objective problems into a single

representative unit called as GRG. The first step of GRA was to normalize the data based on their corresponding objective problem.

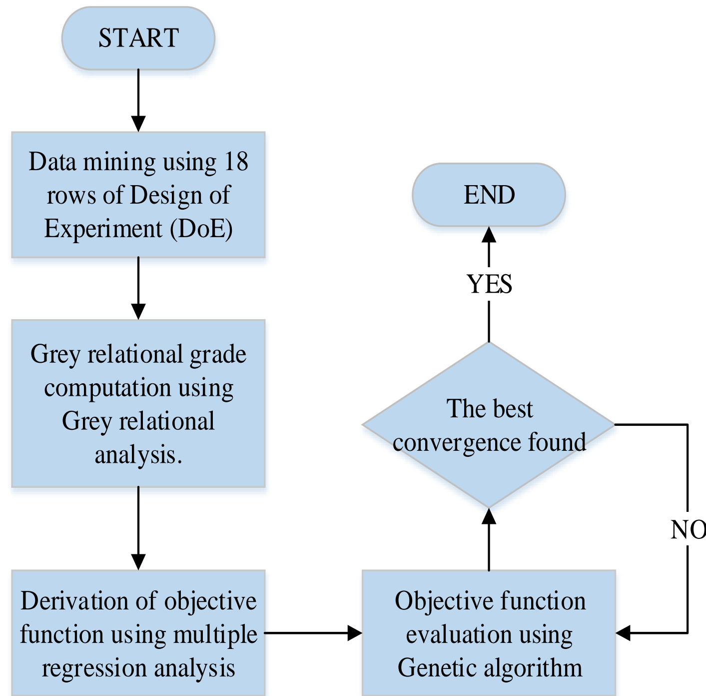

Fig. 2. General flowchart of the predictive analytics.

Table 2. Design parameters and their levels

Symbol	Parameter	Unit	Level		
			Low	**Medium**	**High**
x_1	Ge mole fraction in SiGe layer	-	0.1 (10%)	0.2 (20%)	0.3 (30%)
x_2	High-k material Thickness, $T_{high\text{-}k}$	nm	1	2	3
x_3	S/D Doping, N_{sd}	cm^{-3}	1×10^{13}	2×10^{13}	3×10^{13}
x_4	Metal Workfunction (*WF*)	eV	4.6	4.7	4.8

In this study, the I_{ON}, *on-off ratio*, g_m, f_T and f_{max} were categorized into higher-the-better type of problem in which their magnitudes were expected to be as higher as possible. On the other hand, the I_{OFF} was categorized into lower-the-better type of problem in which its magnitude was expected to be as lower as possible. Thus, the magnitude of all the electrical characteristics with their respective problems for each row can be normalized as follows:

$$x_i^*(k) = \frac{x_i(k) - \min x_i(k)}{\max x_i(k) - \min x_i(k)}, higher - the - better \quad (6)$$

$$x_i^*(k) = \frac{\max x_i(k) - x_i(k)}{\max x_i(k) - \min x_i(k)}, lower - the - better \quad (7)$$

for which $x_i*(k)$ and $x_i(k)$ are the sequence after data normalization and comparability sequence. Next, the deviation sequence, $\Delta oi(k)$ for each experimental row was calculated as follows:

$$\Delta_{oi}(k) = |x_o^*(k) - x_i^*(k)| \quad (8)$$

for which $xo*(k)$ is the reference sequence which is commonly fixed to 1. With the computed deviation sequences, the Grey relational coefficient (GRC), $\xi(k)$ can be then calculated as:

$$\xi(k) = \frac{\Delta_{min} + \xi\Delta_{max}}{\Delta_{oi}(k) + \xi\Delta_{max}} \quad (9)$$

for which ξ, Δ_{max} and Δ_{min} stand for an identification coefficient, a maximum absolute difference and a minimum absolute difference respectively. Since all the investigated design parameters were equally preferred, the magnitude of ξ was fixed to 0.5. Finally, the GRG of each experimental row can be calculated by taking an average magnitude of the GRC for each investigated electrical characteristics. Since the number of the investigated electrical characteristics was six, the GRG, γ_i can be measured as:

$$\gamma_i = \frac{1}{6}[\xi_1 + \xi_2 + \xi_3 + \xi_4 + \xi_5 + \xi_6] \quad (10)$$

After determining the GRG for all the 18 experimental rows, the GRGs can be analysed using multiple regression analysis which will be comprehensively explained in the next section.

3.2. Multiple regression analysis

Multiple regression analysis is commonly utilized to describe the interrelationship between and two or more independent inputs and one dependant output. The main objective of the multiple regression analysis is to attain the objective function that represents the relationship between multiple design parameters and the GRG. Thus, with four independent variables (Ge mole fraction, T_{high-k}, N_{sd} and WF), the multiple regression equation for this study can be written as:

$$Y = a + b_1x_1 + b_2x_2 + b_3x_3 + b_4x_4 + e \quad (11)$$

for which Y is an observed score of the dependent variable (GRG), a is the intercept, b is the slope, x is an observed score on the independent variables (Ge mole fraction, T_{high-k}, N_{sd} and WF) and e is an error. In order to perform prediction of a and b magnitude, the error term (e) will be neglected, thereby the previous equation can be simplified as:

$$Y = a + b_1x_1 + b_2x_2 + b_3x_3 + b_4x_4 \quad (12)$$

Determining the magnitude of regression coefficients (a, b_1, b_2, b_3, b_4) are quite complicated especially when the regression model consists of more than two independent variables. Thus, it requires the application of some complicated and long matrix formulation. In this study, the computation of b and a magnitudes were solved by using an integrated development environment (IDE), Rstudio. After determining the magnitude of a, b_1, b_2, b_3 and b_4, the objective function of the multiple regression model can be further analysed using Genetic Algorithm (GA) which will be briefly described in the subsequence section.

3.3. Genetic algorithm

Genetic Algorithm (GA) is a type of partial search algorithm inspired by the process of natural selection. It reflects the process of natural selection in which the fittest individuals are chosen for reproduction of the future offspring generation. In this study, the GA was employed after retrieving the objective function. Optimization using GA initiated with a population that was randomly generated and it was continually altered over iterations by subsequent operations such as fitness evaluation, selection, crossover and mutation. The initial population represents the initial magnitudes of the design parameters in which each of them is regarded as an individual. In this study, the design parameters (Ge mole fraction, $T_{high\text{-}k}$, N_{sd} and *WF*) were kept as real magnitudes. The objective function evaluation was conducted during the previous section using multiple regression analysis. After that, the objective function was converted into a scaled magnitude within a specific upper and lower boundary, known as fitness function (f_i). The optimum performance of the device was implied by the highest GRG in which the fitness function was required to be maximized. Since, the algorithm was purposely designed for searching the minima of function, it was then converted into the maximization problem by inverting the objective function. Hence, the fitness function for this study can be formulated as:

Minimize $-f(x_1, x_2, x_3, x_4)$
Subject to the constraints:
$0.1 \leq x_1 \leq 0.3$
$1 \leq x_2 \leq 3$
$1 \leq x_3 \leq 3$
$4.6 \leq x_4 \leq 4.8$

Multiple good solutions were then selected while the bad solutions were proportionally removed from the population by maintaining the size of population constant. Since the average fitness of the entire population was denoted as f_{avg}, it can be assumed that a solution with a fitness, f_i did attain an expected f_i/f_{avg} number of copies in the mating pool. Next, two parent strings were randomly selected from the mating pool and their respective string parts were interchanged between two randomly selected crossover points for new generation of children strings with pre-determined crossover probability. After reproduction and the crossover with pre-determined mutation probability, new strings called mutation children were generated by slightly random changes of individuals in the modified population. The computation iterated until there was no further improvement in the best fitness value for a certain number of cycle generations. At this point, the number of iterations were terminated as the best fitness value was identified. Finally, the new populations (Ge mole fraction, $T_{high\text{-}k}$, N_{sd} and *WF*) were successfully predicted. The GA approach for this study was also conducted using Rstudio IDE. The GA settings for this study were pre-determined as below:

Type = *real-valued*
Population size = 50
Number of generations = 1000
Elitism = 2
Crossover probability = 0.8
Mutation probability = 0.1

4. Results and Discussion

Simulation results for 18 sets of experiment were recorded as listed in Table 3. The actual magnitudes of all the investigated characteristics were retrieved based on the design parameter levels allocated to their respective experimental rows. The actual magnitudes of I_{ON}, I_{OFF}, *on-off ratio*, g_m, f_T and f_{max} were normalized in accordance with their respective objective problem using eq. (6) and eq. (7). The deviation sequences for each experimental rows were subsequently measured using eq. (8). The magnitudes of the deviation sequences for each row were then employed to calculate the Grey relational coefficients (GRC) by using eq. (9).

Table 3. Simulation results for 18 sets of experiment

Exp.	I_{ON} (μA/μm)	I_{OFF} (nA/μm)	On-off ratio (x10^5)	g_m (mS/μm)	f_T (GHz)	f_{max} (THz)
1	1182.9	2.77	4.3	1.91	124.9	1.7
2	992	8.34	1.2	2.42	221.8	2.8
3	1022.2	17.2	0.6	3.29	515.6	7
4	1682.2	3.13	5.4	3.06	397.1	5
5	1612.6	1.58	10.2	3.63	597.3	8.1
6	1249.7	4.34	2.9	3.56	638.6	9.5
7	1200.2	15.9	0.8	2.11	415.2	7
8	989.1	3.96	2.5	2.37	465	7.7
9	998.6	5.2	1.9	2.78	519.8	8.3
10	1617.5	6.49	2.5	2.4	147.5	1.9
11	1618.3	14.8	1.1	3.37	281.2	3.2
12	1281.3	36.3	0.4	3.86	564.6	7.3
13	1391.5	14	1	2.3	332.5	4.8
14	1161.2	31.7	0.4	2.59	489.3	7.5
15	1181.2	52.2	0.2	3.46	632	9.5
16	1669.9	27.7	0.6	2.97	526.2	7.8
17	1589.7	8.58	1.9	3.39	599	8.7
18	1250.5	15.2	0.8	3.23	580	8.7

Since there were six design parameters involved in the current study, the Grey relational grades (GRG) for each row were determined by averaging the respective GRC by six. The GRGs for all the experimental rows were recorded as listed in Table 4. The GRGs for each row were ranked based on the highest magnitude. The higher GRG indicated that the respective experimental row had a better quality of multiple electrical characteristics. The calculated GRGs for each experimental rows were then analysed using multiple regression analysis in order to derive the objective function.

The magnitude of estimated regression coefficients (a, b_1, b_2, b_3, b_4) were determined with the aid of Rstudio IDE. A normal probability plot of MRA for the calculated GRGs are depicted in Fig. 3.

It shows the variation of the GRGs on the estimated regression line. Table 5 shows the summary of the multiple regression analysis for this study. It is clearly shown that the most significant design parameter contributing the large variation on the GRG magnitude is parameter x_3 (S/D doping). On the other hands, the least significant design parameter is identified as parameter x_4 (workfunction).

Table 4. Grey relational grades and ranks.

Exp. No.	GRG (γi)	Rank
1	0.470586	17
2	0.438925	18
3	0.536961	12
4	0.66358	4
5	0.873202	1
6	0.752953	2
7	0.484357	15
8	0.552922	11
9	0.585021	9
10	0.526141	13
11	0.553642	9
12	0.606464	8
13	0.476852	16
14	0.486938	14
15	0.626598	5
16	0.619188	6
17	0.719926	3
18	0.615692	7

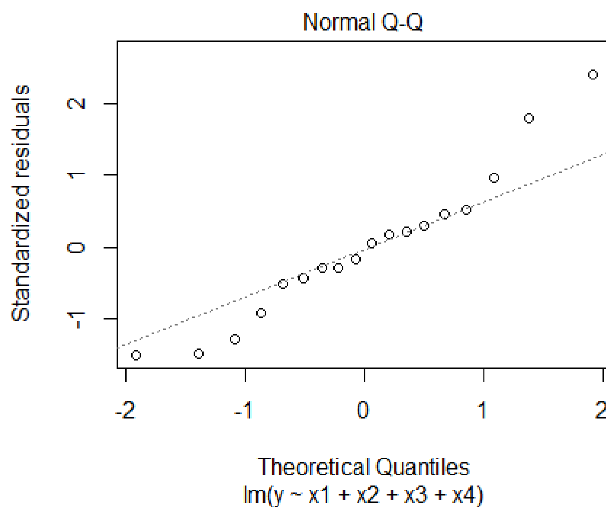

Fig. 3. Normal probability plot.

Table 5. Results of multiple regression analysis.

Regression Coefficients	Estimation	Std. Error	t value	Pr (>|t|)	Significant code
Intercept	0.98525	0.99031	0.995	0.337948	
x1	-0.45912	0.21490	-2.136	0.052238	.
x2	0.05999	0.02149	2.791	0.015279	*
x3	0.10776	0.02149	5.014	0.000237	***
x4	-0.13629	0.21490	-0.634	0.536944	
Significant Code: 0 ‘*’, 0.001 ‘**’, 0.01 ‘*’, 0.05 ‘.’ 0.1-1 ‘ ’**					

Based on the estimated regression coefficients in Table 5, the objective function for the GRG distributions can be mathematically described as:

$$Y = 0.98525 - 0.45912x_1 + 0.05999x_2 + 0.10776x_3 - 0.13629x_4 \quad (13)$$

Since GA was originally developed to find the local minima of a function, the objective function was then inverted into a fitness function within a specific upper and lower boundary as follows:

$$Y = -0.98525 + 0.45912x_1 - 0.05999x_2 - 0.10776x_3 + 0.13629x_4 \quad (14)$$

As can be observed, the sign of the initial objective function is inverted to allow the GA solving the maximization based problems in which the GRG is desired to be as large as possible. The inverted fitness function was then optimized using GA. The search for the optimum fitness function ended after 367 generations as the best fitness value was identified. The computational runtime of the hybrid model, with respect to the 367 cycles of generation only took about 5 seconds, predominantly due to less complexity of the small datasets. Figure 4 depicts the plot of the fitness function in each generation as the numbers of generation converge at the optimum point. The final results of GA optimization are summarized in Table 6.

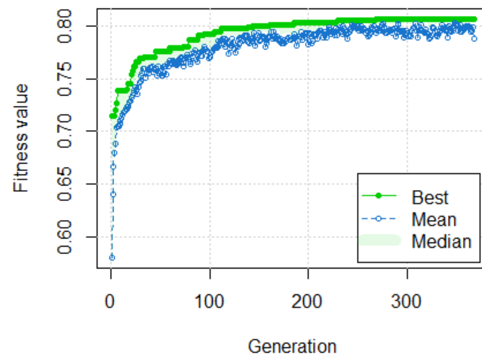

Fig. 4. Performance of GA during convergence.

Table 6. Summary of the final results of genetic algorithm.

Parameters	Magnitude and its unit
Optimum GRG	0.8070043
Ge mole fraction in SiGe layer	0.1 (10%)
High-k material Thickness, T_{high-k}	3 nm
S/D Doping, N_{sd}	3×10^{13} cm^{-3}
Metal Workfunction (*WF*)	4.6 eV

It is observed that the maximum GRG is measured at 0.8070043 which can be attained by employing the design parameters; Ge mole fraction, T_{high-k}, N_{sd} and *WF* with their predicted magnitudes of 0.1 (low), 3 nm (high), 3×10^{13} cm^{-3} (high) and 4.6 eV (low) respectively. However, the previous DoE (Table 2) does not include the predicted magnitudes of the design parameter. Hence, the simulation of the device needs to be redone for verification purpose.

Figure 5 shows an overlay plot of I_{ds}-V_{gs} transfer characteristic before and after predictive analytics. It can be observed that the I_{ON} magnitude of the device is improved

by ~34% after the predictive analytics. Larger I_{ON} is definitely required for nano-scale device especially when being involved in high speed switching application.

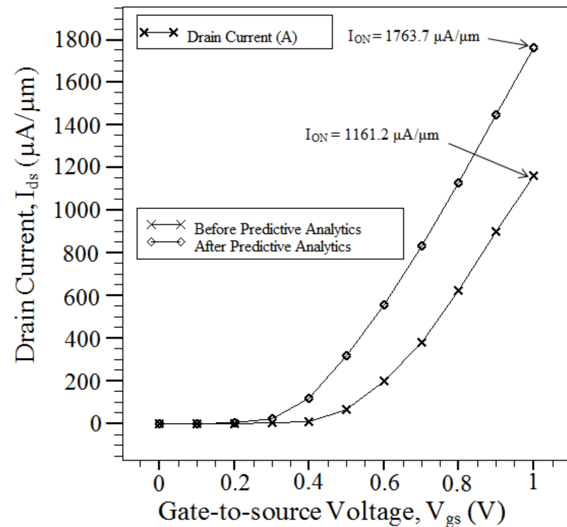

Fig. 5. Overlay plot of the I_{ds}-V_{gs} curve before and after predictive analytics in linear mode.

The rest of the examined transistor characteristics can be determined using the aforementioned equations. Figures 6 and 7 show the comparison of the I_{OFF} magnitude and the *on-off ratio* of the device before and after predictive analytics respectively. It can be seen that the I_{OFF} magnitude of the device is reduced by ~40% after the predictive analytics. A large I_{OFF} magnitude would definitely affect the standby power of the device, thereby increasing the power consumption. Meanwhile, the *on-off ratio* of the device is improved by ~50% after the predictive analytics as depicted in Fig. 9. The larger *on-off ratio* implies that the device has better power consumption as much minimum V_{gs} is required to drive the I_{ds} reach its saturation.

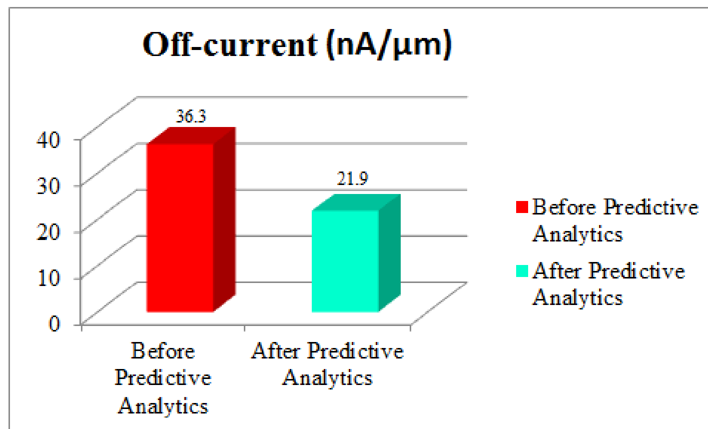

Fig. 6. Bar Graph of I_{OFF} before and after predictive analytics.

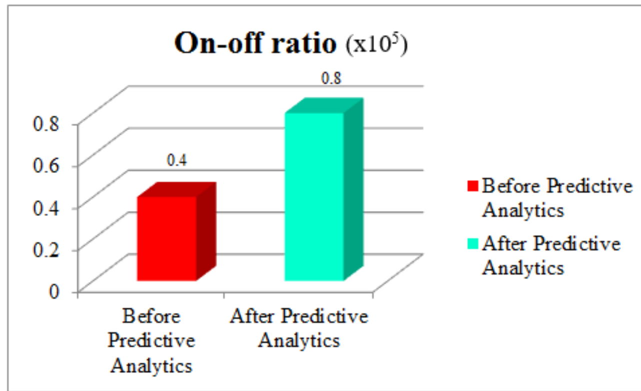

Fig. 7. Bar Graph of On-off ratio before and after predictive analytics.

Figure 8 depicts an overlay plot of g_m against V_{gs} before and after predictive analytics. From the plot, it can be observed that the g_m magnitude of the device at maximum V_{gs} is improved by ~18% after the predictive analytics. Gaining a much higher g_m magnitude is very crucial for the device to operate as a transconductance amplifier. In fact, a higher g_m magnitude would boost the intrinsic gain as well as the device efficiency. Figure 9 depicts an overlay plot of f_T against V_{gs} before and after predictive analytics. From the plot, it can be observed that the f_T magnitude of the device at maximum V_{gs} is slightly improved by ~10% after the predictive analytics. This indicates that the device would be capable of amplifying much higher input signal after going through the predictive analytics. Figure 10 depicts an overlay plot of f_{max} against V_{gs} before and after predictive analytics. The f_T magnitude of the device at maximum V_{gs} is observed to be slightly improved by ~4% after the predictive analytics. A higher f_{max} magnitude could boost an achievable maximum power gain of the device. Based on the overall results, it can be concluded that the proposed predictive analytics are capable of optimizing the investigated design parameters (Ge mole fraction, $T_{high\text{-}k}$, N_{sd} and *WF*) in attaining better device characteristics (I_{ON}, I_{OFF}, *on-off ratio*, g_m, f_T and f_{max}).

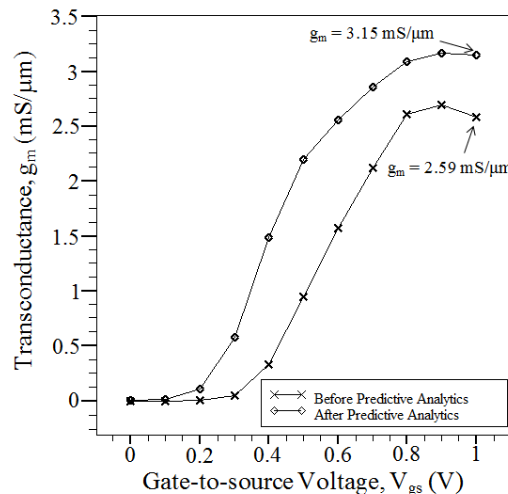

Fig. 8. Overlay plot of the g_m-V_{gs} curve before and after predictive analytics.

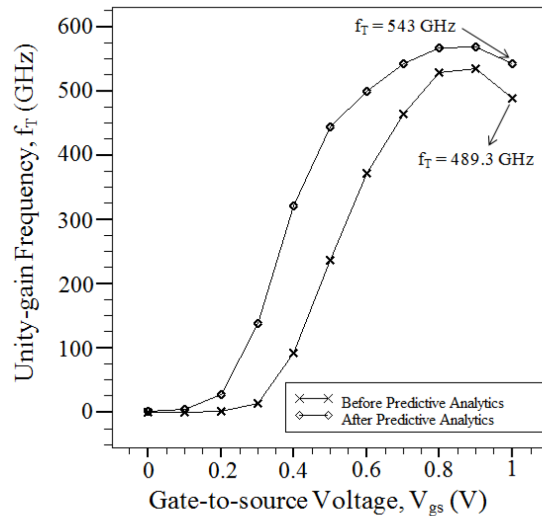

Fig. 9. Overlay plot of the f_T-V_{gs} curve before and after predictive analytics.

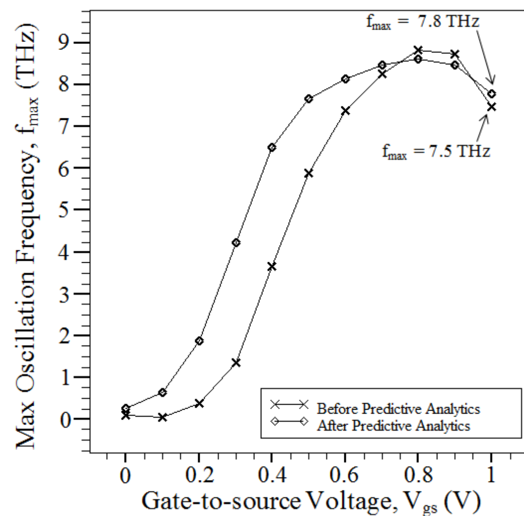

Fig. 10. Overlay plot of the f_{max}-V_{gs} curve before and after predictive analytics.

Table 7 summarizes all of the observations on transistor characteristics before and after predictive analytics. It can be clearly seen that the I_{OFF} magnitude of the device is reduced by ~40% after the predictive analytics. A large I_{OFF} magnitude would definitely affect the standby power of the device, thereby increasing the power consumption. Meanwhile, the *on-off ratio* of the device is improved by ~50% after the predictive analytics. The larger *on-off ratio* implies that the device has better power consumption as much minimum V_{gs} is required to drive the I_{ds} reach its saturation. It is observed that the g_m magnitude of the device at maximum V_{gs} is improved by ~18% after the predictive analytics. Gaining a much higher g_m magnitude is very crucial for the device to operate as a transconductance amplifier. In fact, a higher g_m magnitude would boost the intrinsic gain as well as the device efficiency.

Table 7. Comparison of simulation results before and after predictive analytics.

JLDGSM's Parameter/characteristic	Before predictive analytics	After predictive analytics
Ge mole fraction in SiGe layer	0.3 (30%)	0.1 (10%)
High-k material Thickness, (T_{high-k})	2 nm	3 nm
S/D Doping (N_{sd})	1×10^{13} cm^{-3}	3×10^{13} cm^{-3}
Metal Workfunction (WF)	4.7 eV	4.6 eV
On-current (I_{ON})	1161.2 μA/μm	1763.7 μA/μm
Off-current (I_{OFF})	36.3 nA/μm	21.9 nA/μm
On-off ratio	0.4×10^5	0.8×10^5
Transconductance (g_m)	2.59 mS/μm	3.15 mS/μm
Unity-gain frequency (f_T)	489.3 GHz	543 GHz
Max. oscillation frequency (f_{max})	7.5 THz	7.8 THz

The f_T magnitude of the device at maximum V_{gs} is slightly improved by ~10% after the predictive analytics. This indicates that the device would be capable of amplifying much higher input signal after going through the predictive analytics. Furthermore, the f_{max} magnitude of the device at maximum V_{gs} is observed to be slightly improved by ~4% after the predictive analytics. A higher f_{max} magnitude could boost an achievable maximum power gain of the device. Based on the overall results, it can be concluded that the proposed predictive analytics are capable of optimizing the investigated design parameters (Ge mole fraction, T_{high-k}, N_{sd} and WF) in attaining better device characteristics (I_{ON}, I_{OFF}, *on-off ratio*, g_m, f_T and f_{max}). For comparison with other state-of-art, some results produced by the proposed hybrid predictive analytics are compared with previous works as detailed in Table 8.

Table 8. Comparison with other state-of-art transistor models.

Research work	Year	L_g (nm)	I_{ON} (μA/μm)	g_m (mS/μm)	f_T (GHz)
Ajayan et al. [30]	2019	12	250	0.39	369
Suddapalli and Nistala [31]	2020	20	1500	4	795
Rashid et al. [32]	2021	20	123.1	1.23	100
Sreenivasulu and Narendar [33]	2021	18	59.7	0.9	450
Raut and Nanda [34]	2021	30	10	4	546.54
Misra et al. [35]	2022	30	226.8	0.23	536
fKumar et al. [36]	2022	30	44	0.069	44
This work	2023	6	1763	3.15	543

All previous transistor models have already used ultra-thin channel either in double-gate or single-gate structure, or they have been improved or hybridized with other innovations. Comparable to earlier transistor models, our recent research has showed good device characteristics with high I_{ON}, g_m, and f_T. In addition, our research focuses on reducing the physical gate length to 6nm while maintaining acceptable device performance via the use of strain, high-k/metal-gate engineering, and predictive analytics. The main limitation of the proposed predictive analytics

model is it may not guarantee that a globally optimal solution can be reached on every type of problems. Furthermore, metaheuristics such as Genetic algorithm will never reach an optimum point, if the optimisation problem is too complex and/or very large. Hence, it is necessary to implement and introduce new algorithm that is more suitable for the existing problems. The sensitivity of the optimized parameters to variations in process technology or potential trade-offs between different device's characteristics is very crucial in transistor's performance. Based on previous multiple regression analysis, S/D doping process was recognized the main design parameter that contributed the most impact on the variations of device's characteristics. Table 9 shows the impact of the S/D doping (N_{sd}) variations on JLDGSM's characteristics (Note: Other parameters are set to the optimum level predicted by predictive analytics approach).

Table 9. Summary of the N_{sd} variations on JLDGSM's characteristics.

N_{sd} (cm^{-3})	*Ion* (μA/μm)	I_{off} (nA/μm)	*On-off* ratio	g_m (mS μm)	f_T (GHz)	f_{max} (THz)
1×10^{13}	1149.8	13.0	0.88× 10^5	2.12	417	7.0
2×10^{13}	1518.9	17.5	0.87× 10^5	2.84	503	7.5
3×10^{13}	1763.7	21.9	0.8× 10^5	3.15	543	7.8

Based on Table 9, the N_{Sd} parameter is directly proportional to all the investigated JLDGSM's characteristics in which it exhibit increasing trend in I_{ON}, I_{OFF}, *on-off ratio*, g_m, f_T and f_{max} as the N_{sd} is increased. Hence, the N_{sd} parameter need to be carefully tuned as it might contribute significant trade-offs of the overall JLDGSM's performance. In future work, more design parameters besides Ge mole fraction, $T_{high\text{-}k}$, N_{sd} and *WF* will be taken into account for more comprehensive perspective.

5. Conclusions

In the present work, a hybrid model of predictive analytics involving Grey Relational Analysis (GRA) and Genetic Algorithm (GA) are developed and utilized for prediction and optimization of the Ge mole fraction (Ge Mole), high-*k* material thickness ($T_{high\text{-}k}$), source/drain (S/D) doping concentration and metal work-function (*WF*) of n-type Junctionless Double Gate Strained MOSFET (JLDGSM). The GRA is mainly employed to merge all the design parameters with different objective problem into a single representative unit called Grey Relational Grade (GRG). The computed GRGs are then analysed using multiple regression analysis in order to derive the objective function. The GA is applied by scaling the objective function into fitness function restricted to pre-determined upper and lower boundaries. The best fitness value is identified after 367 cycles of generation. Based on the final results, the proposed predictive analytics have successfully optimized I_{ON}, I_{OFF}, *on-off ratio*, g_m, f_T and f_{max} of the device by ~34%, ~40%, ~50%, ~18%, ~10% and ~4% respectively. The best combinational magnitudes of Ge mole fraction, $T_{high\text{-}k}$, N_{sd} and *WF* for the most optimum device characteristics are predicted to be 0.1 (10%), 3 nm, 3×10^{13} cm^{-3} and 4.6 eV respectively. It can be concluded that the proposed predictive analytics are capable of optimizing multiple design parameters for much improved JLDGSM performance.

Acknowledgement

This work was supported by Ministry of Higher Education (MOHE) under research grants (FRGS/1/2022/TK07/UTEM/02/47) and CeTRI, FTKEK, Universiti Teknikal Malaysia Melaka (UTeM).

Nomenclatures

a	Intercept
b	Slope
C_{gd}	Gate-to-drain capacitance
C_{gs}	Gate-to-source capacitance
Ge	Germanium
f	Frequency
f_{avg}	Average fitness
f_i	Fitness function
f_{max}	Maximum oscillation frequency
f_T	Unity-gain frequency
g_m	Transconductance
HfO_2	Hafnium dioxide
I_{ds}	Drain-to-source current
I_{OFF}	Off-state current
I_{on}	On-state current
L_g	Physical gate length
Nc	Channel doping concentration
N_{sd}	Source/drain doping concentration
$T_{high\text{-}k}$	High-k material thickness
t_{ox}	Gate oxide thickness
t_{si}	Silicon film thickness
V_{ds}	Drain-to-source voltage
V_{gs}	Gate-to-source voltage
WSi_x	Tungsten silicide
x	Observed score on the independent variables
$x_i*(k)$	Sequence after data normalization
$x_i(k)$	Comparability sequence
$xo*(k)$	Reference sequence

Greek Symbols

Δ_{max}	Maximum absolute difference
Δ_{min}	Minimum absolute difference
$\Delta oi(k)$	Deviation sequence
ξ	Identification coefficient
$\xi(k)$	Grey relational coefficient
γ_i	Average magnitude of the Grey relational coefficients

Abbreviations

AC	Alternate current
DC	Direct current
DoE	Design of experiments

DIBL	Drain induced barrier lowering
GA	Genetic algorithm
GAA	Gate all around
GRA	Grey relational analysis
GRC	Grey relational coefficient
GRG	Grey relational grade
JLDGSM	Junctionless double gate strained MOSFET
RF	Radio frequency
RSM	Response surface methodology
S/D	Source/drain
SS	Subthreshold slope
TCAD	Technology computer aided design
WF	Workfunction

References

1. Swami, Y.; and Rai, S. (2021). Physical parameter variation analysis on the performance characteristics of nano DG-MOSFETs. *Circuits and Systems*, 12(4), 39-53.
2. Bala, S.; and Kumar, A. (2022). Parameter variation analysis of dopingless and junctionless nanotube MOSFET. *Silicon*, 14(10), 5255-5263.
3. Batakala, J.; and Dhar, R.S. (2022). Effect of channel material on the performance parameters of GAA MOSFET. *Journal of Nano- and Electronic Physics*, 14(2), 1-5.
4. Wagaj, S.C.; and Patil, B.B. (2022). Simulation of graded channel double gate junctionless transistor for low power and high performance. *International Advanced Research Journal in Science*, *Engineering and Technology*, 9(4), 251-260.
5. Sinha, S.K. (2021). Performance assessment of double gate graded junction-less-FET device with temperature variations. *International Journal of Nanoparticles*, 13(1), 33-41.
6. Hoeneisen, B.; and Mad, C.A. (1972). Fundamental limitation in microelectronics -I.MOS technology. *Solid-State Electronics*, 15, 819-829.
7. Asenov, A. (1998). Statistically reliable 'Atomistic' simulation of Sub 100nm MOSFETs. *Simulation of Semiconductor Process and Devices*, 223-226.
8. Asenov, A.; Brown, A.R.; Davies, J.H.; Kaya, S.; and Slavcheva, G. (2003). Simulation of intrinsic parameter fluctuations in decananometer and nanometer-scale MOSFETs. *IEEE Transactions on Devices*, 50(9), 1837-1852.
9. Asenov, A.; and Kaya, S. (2000). Effect of oxide interface roughness on the threshold voltage fluctuations in decanano MOSFETs with ultrathin gate oxides. *International Conference on Simulation of Semiconductor Processes and Devices*, September, 135-138.
10. Ghosh, P.; and Bhomick, B. (2022). Study of variability induced by random dopant fluctuation in Fe DS-SBTFET. *Microelectronics Journal*, 125, 105467.
11. Kim, K.Y.; and Park, B.-G. (2021). Effect of random dopant fluctuation on data retention time distribution in DRAM. *IEEE Transactions on Electron Devices*, 68(11), 5572-5577.

12. Lee, S.; Yoon, J.; Lee, J.; Jeong, J.; Yun, H., Lim, J.; Lee, S.; and Baek, R. (2022). Novel modeling approach to analyze threshold voltage variability in short gate-length (15-22 nm) nanowire FETs with various channel diameters. *Nanomaterials*, 12(10), 1721.
13. Ramesh, R.; Pon, A.; Babu, P.D.; Carmel, S.; and Bhattacharyya, A. (2022). Optimization of gate all-around junctionless transistor using response surface methodology. *Silicon*, 14(6). 2499-2508.
14. Sundaramk, M.; Prakash, P.; Angaleswari, S.; Deepa, T.; Natrayan, L.; and Paramasivam, P. (2021). Influence of process parameter on carbon nanotube field effect transistor using response surface methodology. *Journal of Nanomaterials*, 2021(7739359), 1-9.
15. Roslan, A.F.; Salehuddin, F.; Zain, A.S.M.; Kaharudin, K.E.; Ahmad, I.; Hazura, H.; Hanim, A.R.; Idris, S.K.; and Afifah Maheran, A.H. (2020). Optimization of process parameter variations for 16nm DG-FinFET using Response Surface Methodology-Central Composite Design. *Journal of Physics: Conference Series*, 1502, 012042.
16. Williams, S.; and Varahramyan, K. (2000). A new TCAD-based statistical methodology for the optimization and sensitivity analysis of semiconductor technologies. *IEEE Transactions on Semiconductor Manufacturing*, 13(2), 208-218.
17. Izwanizam, Y.; Afifah Maheran, A.H.; Salehuddin, F.; and Kaharudin, K.E. (2022). Optimization of 22nm Bi-GFET device for threshold voltage using Taguchi method Optimization of 22nm Bi-GFET device for threshold voltage using Taguchi method. *AIP Conference Proceedings*, 040004(June), 1-8.
18. Othman, N.A.F.; Azhari, F.N.N.; Hatta, S.F.W.M.; and Soin, N. (2018). Optimization of 7 nm strained germanium FinFET design parameters using Taguchi method and pareto analysis of variance. *ECS Journal of Solid State Science and Technology*, 7(4), P161-P169.
19. Mah, S.K.; Ahmad, I.; Ker, P.J.; Tan, K.P.; and Faizah, Z.A.N. (2018). Modeling, simulation and optimization of 14nm high-K/metal gate NMOS with Taguchi method. *IEEE International Conference on Semiconductor Electronics*, *Proceedings*, August, 275-278.
20. Kaharudin, K.E.; Salehuddin, F.; Zain, A.S.M.; Aziz, M.N.I.A.; and Ahmad. I. (2016). Application of Taguchi method for lower subthreshold swing in ultrathin pillar SOI VDG- MOSFET device. *Journal of Advanced Research in Applied Sciences and Engineering Technology*, 2(1), 30-43.
21. Kulkarni, S.S.; Konnur, V.S.; and Ganjigatti, J.P. (2022). Optimization of MIG welding process parameters with grey relational analysis for AL 6061 alloy. *Welding International*, 36(7), 387-393.
22. Gong, T.; Wu, Y.; Li, J.; Lin, W.; Gao. L.; Shen, L.; Zhao, N.; and Ming, T; (2022). A system level optimization of on-chip thermoelectric cooling via Taguchi-Grey method. *Applied Thermal Engineering*, 214, 118845.
23. Mukherji, D.; Ranjan, R.; and Moi, S.C. (2022). Multi-response optimization of surface roughness and MRR in turning using Taguchi grey relational analysis (TGRA). *International Research Journal of Multidisciplinary Scope*, 3(2), 1-7.

24. Kaharudin, K.E.; and Salehuddin, F. (2022). Predictive modeling of mixed halide perovskite cell using hybrid L27 OA Taguchi-based GRA-MLR-GA approach. *Jurnal Teknologi*, 1(84), 1-9.
25. Fan, J.; Qian, Y.; Chen, W.; Jiang, J.; Tang, Z.; Fan, X; and Zhang, G. (2022). Genetic algorithm-assisted design of redistribution layer vias for a fan-out panel-level SiC MOSFET Power Module Packaging. *IEEE* 72*nd Electronic Components and Technology Conference* (*ECTC*), 260-265.
26. Sarvaghad-Moghaddam, M.; Orouji, A.; Ramezani, Z.; Elhoseny, M.; Farouk, A.; and Arun Kumar, N. (2019). Modelling the spice parameters of SOI MOSFET using a combinational algorithm. *Cluster Computing*, 22, 4683-4692.
27. Kaharudin, K.E.; Salehuddin, F.; Zain, A.S.M.; Roslan, A.F.; and Ahmad, I. (2021). Work function variations on electrostatic and RF performances of JLSDGM Device. *Indonesian Journal of Electrical Engineering and Computer Science*, 23(1), 150-161.
28. Ju-long, D. (1982). Control problems of grey systems. *Systems and Control Letters*, 1(5), 288-294.
29. Kaharudin, K.E.; Salehuddin, F.; Zain, A.S.M.; Aziz, M.N.I.A.; Manap, Z.; Salam, N.A.A.; and Saad, W.H.M. (2016). Design and optimization of $TiSi_x/HfO_2$ channel vertical double gate NMOS device. *IEEE International Conference on Semiconductor Electronics*, 69-73.
30. Ajayan, J.; Nirmal, D.; Kurian, D.; Mohankumar, P.; Arivazhagan, L., Augustine Fletcher, A.S.; Subash, T.D.; and Saravanan, M. (2019). Investigation of impact of gate underlap/overlap on the analog/RF performance of composite channel double gate MOSFETs. *Journal of Vacuum Science & Technology B*, 37(6), 062201.
31. Suddapalli, S.R.; and Nistala, B.R. (2020). The analog/RF performance of a strained-Si graded-channel dual-material double-gate MOSFET with interface charges. *Journal of Computational Electronics*, September 1-11.
32. Rashid, S.; Bashir, F.; Khanday, F.A.; Rafiq Beigh, M.; and Hussin, F.A. (2021). 2-D Design of double gate Schottky tunnel MOSFET for high-performance use in analog/rf applications. *IEEE Access*, 9, 80158-80169.
33. Sreenivasulu, V.B.; and Narendar, V. (2021). Design insights into RF/analog and linearity/distortion of spacer engineered multi-fin SOI FET for terahertz applications. *International Journal of RF and Microwave Computer-Aided Engineering*, 31(12), 1-14.
34. Raut, P.; and Nanda, U. (2021). RF and linearity parameter analysis of junction-less gate all around (JLGAA) MOSFETs and their dependence on gate work function. *Silicon*, 14, 5427-5435.
35. Misra, S.; Biswal, S.M.; Baral, B.; Swain, S.K.; and Pati, S.K. (2022). Study of analog/Rf and stability investigation of surrounded gate junctionless graded channel MOSFET(SJLGC MOSFET). *Silicon*, 14, 6391-6402.
36. Kumar, P.; Koley, K.; Mech, B.C.; Maurya, A.; and Kumar, S. (2022). Analog and RF performance optimization for gate all around tunnel FET using broken-gap material. *Scientific Reports*, 12(1), 1-15.